ELSEVIER

PII: S0032-3861(97)10182-3

Polymer Vol. 39 No. 18, pp. 4279–4287, 1998

0032-3861/98/$19.00+0.00

Tensile drawing of ethylene/vinyl alcohol copolymers: II. Investigation of the strain-induced mesomorphic structure

Laurence Penel[a], Karina Djezzar[a], Jean-Marc Lefebvre[a], Roland Séguéla[a,*] and Hubert Fontaine[b]

[a]*Laboratoire 'Structure et Propriétés de l'Etat Solide' URA CNRS 234, Université des Sciences et Technologies de Lille, Bât. C6, 59655 Villeneuve d'Ascq, Cedex, France*
[b]*Laboratoire 'Dynamique et Structures des Matériaux Moléculaires' URA CNRS 801, Université des Sciences et Technologies de Lille, Bât. P5, 59655 Villeneuve d'Ascq, Cedex, France*
(Received 14 February 1997; revised 23 June 1997; accepted 20 August 1997)

The structural modifications of ethylene/vinyl alcohol copolymers under tensile drawing are investigated as a function of draw temperature and draw ratio. By combining wide-angle and small-angle X-ray scattering, it is shown that a mesomorphic-like structure develops from the original crystalline phase for draw temperatures below 110°C and draw ratios beyond $\lambda = 4$. Thermal analysis indicates that the resulting strain-induced disordered phase reorganises into the stable monoclinic form above 110°C. Annealing treatments reveal that the thermal stability of the new phase is directly connected to the α mechanical relaxation. X-ray and thermal investigations on quenched samples show that the mesomorphic crystalline form can be induced in the isotropic state. A hexagonal unit cell with random distribution of the hydrogen bonds about the chain axis owing to conformational disorder is proposed. A mechanism of crystalline phase modification is discussed in terms of transverse crystallographic slip.

(Keywords: ethylene/vinyl alcohol copolymers; tensile drawing; X-ray scattering)

INTRODUCTION

The solid-state processing of thermoplastic polymers into high-stiffness and high-strength moulded parts has stimulated a great deal of investigations on the uniaxial drawing of semi-crystalline flexible-chain polymers with the aim of understanding the mechanisms of the improvement of both mechanical and physical properties[1–4]. Polyethylene (PE) and isotactic polypropylene (PP) have been by far the most extensively studied materials. However, polymers having higher thermal stability such as poly(ethylene–terephthalate) (PET), polyoxymethylene (POM), polyamides (PA) or poly(vinyl alcohol) (PVOH) have also received increased attention as potential high-performance oriented materials[5–9].

In the first paper of this series[10], we reported on the influence of the draw temperature on the tensile behaviour of two ethylene/vinyl alcohol copolymers. The change of mechanical properties as a function of draw temperature suggests the occurrence of a structural modification during the drawing process below 100°C. The present paper deals with the investigation of the structure of the copolymers as a function of both temperature and draw ratio. Annealing and quenching treatments are also carried out in order to study the thermal stability of the new phase in relation to the α crystalline relaxation.

* To whom correspondence should be addressed

EXPERIMENTAL

The materials studied are two ethylene/vinyl alcohol copolymers (EVOH) from Nippon Gohsei, Soarnol A and Soarnol DC having 44 and 32 mol% ethylene units, respectively. Their characteristics have been already reported in Table 1 of Ref. 10. Cast films about 200 mm thick as well as sheets about 2 mm thick were studied. More details on the preparation conditions are given in the preceding paper[10]. Both kinds of materials were in the monoclinic crystalline form.

The drawing experiments were performed in an Instron tensile testing machine equipped with an air-pulsed oven regulated at ± 1°C. The draw ratio, $\lambda = l/l_0$, was measured on the samples from the spacing of ink marks initially 1.5 mm apart. Dumbbell-shaped samples with gauge dimensions 24 mm × 5 mm were cut off the films and sheets in order to be drawn at various temperatures, at a cross-head speed of 50 mm min^{-1}.

Annealing treatments of unconstrained drawn samples were carried out in a glycerol bath regulated at ±0.5°C. Quenching experiments were achieved in a water bath at 60°C. The molten material was spread over an aluminium foil with a razor blade in order to form a thin film before plunging into the bath.

The thermal properties were investigated by means of differential scanning calorimetry (d.s.c.), using a Perkin–Elmer DCS-7-Delta apparatus. Isotropic as well as drawn samples were stored for two weeks in closed boxes containing freshly regenerated molecular sieves in order to eliminate most of the absorbed water. The heating and

cooling rates were 10° min^{-1} and the sample weight was in the range 5–10 mg. The melting of indium and zinc samples was used to calibrate temperature and heat flow scales at the same heating rate. The crystal weight fraction, X_c, was assessed as previously described[10].

Wide-angle X-ray scattering (W.A.X.S.) and small-angle X-ray scattering (S.A.X.S.) patterns were recorded on a Luzzati–Baro goniometer equipped with two pinhole collimators 0.5 mm in diameter, 250 mm apart. The nickel-filtered Cu–K_α radiation was selected from a Philips tube operated at 40 kV and 20 mA. The sample-to-film distance was 50 mm and 400 mm for W.A.X.S. and S.A.X.S. experiments, respectively. The exposure time was 12 h using AX and Direct Exposure Kodak films for the recording of the W.A.X.S. and S.A.X.S. patterns, respectively. Measurements of W.A.X.S. intensity profiles have been also carried out on a diffractometer provided with a scintillation counter driven by a step-by-step motor in order to record data at every 0.2° over the Bragg angle ranges $15^\circ < 2\theta < 20^\circ$ and $5^\circ < 2\theta < 10^\circ$. The entrance slit determined a beam aperture of 1/30° and the receiving slit was 0.05 mm wide at a sample-to-counter distance of 50 mm.

S.A.X.S. is discussed with regard to the regular stacking of crystalline lamellae in order to follow the orientational behaviour of the lamella normal as a function of strain, while W.A.X.S. accounts for the chain orientation within the crystalline lamellae. Combination of the kinds of information allows a discussion about the deformation mechanisms[11–15]. The S.A.X.S. intensity changes with deformation, which rely on the electron density contrast between the ordered and amorphous phases, is discussed in terms of crystalline structure modification[16].

RESULTS AND DISCUSSION

Structural characterization

The W.A.X.S. and S.A.X.S. patterns of undeformed compression-moulded sheets of both copolymers are shown in *Figure 1*. The W.A.X.S. patterns exhibit the characteristic reflections of the PVOH monoclinic structure rather than those of the orthorhombic PE structure as revealed by the presence of the two inner (100) and (001) reflections in addition to the two strong reflections common to both structures, with the indexes (110) and (200)[17]. This is consistent with the data from Matsumoto *et al.*[18–20] on ethylene vinyl alcohol copolymers covering the whole range of composition. The S.A.X.S. patterns display a unique broad diffraction ring indicative of the regular stacking of the crystal lamellae. But it is worth mentioning that polyethylene of equivalent crystallinity may display several sharp S.A.X.S. orders owing to a highly regular stacking of large lamellae[21].

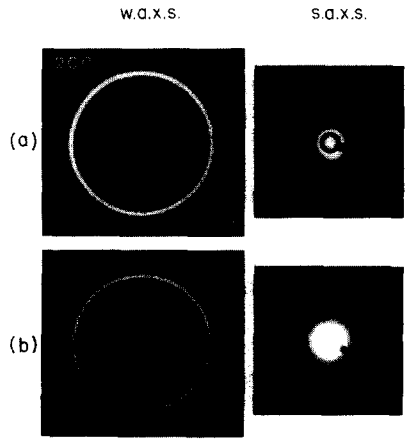

Figure 1 W.A.X.S. and S.A.X.S. patterns of the isotropic (a) copolymer A and (b) copolymer DC

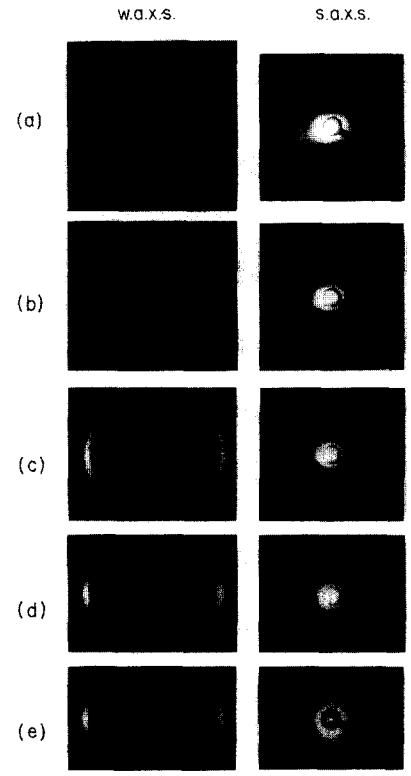

Figure 2 W.A.X.S. and S.A.X.S. patterns of copolymer A for the draw temperature $T_d = 120$°C, as a function of draw ratio: (a) $\lambda = 1.4$, (b) $\lambda = 1.8$, (c) $\lambda = 3.0$, (d) $\lambda = 4.0$, (e) $\lambda = 5.0$ (draw axis vertical)

Figure 2 shows the W.A.X.S. and S.A.X.S. patterns of copolymer A samples drawn at $T_d = 120$°C, as a function of draw ratio. The more intense (110) reflection splits into quadrant arcs at $\lambda = 1.40$ before turning into equatorial arcs for $\lambda \geq 3.0$. The (200) ring already gives equatorial arcs at $\lambda = 1.40$. The azimuthal dispersion decreases with increasing draw ratio. This is quite similar to the crystalline orientational behaviour of PE[14,15]. It is an evidence of the transient oblique orientation of the chains with respect to the draw axis as required for the crystallographic slip of the lamellae, before achieving the classical parallel orientation of the chains in the draw axis after necking. However, beyond $\lambda = 4.0$, the (200) reflection weakens and merges with the (110) reflection into a single broad spot indicating, on the one hand, that the chains are fairly well aligned parallel to the draw direction and, on the other hand, that some disorder takes place in the lateral packing of the oriented chains. The persistence of the inner (100) reflection beyond $\lambda = 4$ reveals that a good part of the monoclinic crystal order is preserved.

The S.A.X.S. unique diffraction order (*Figure 2*) first turns into arched equatorial reflections that are relevant to a preferred orientation of the lamellae towards the draw direction. Considering the oblique orientation of the chains, it comes out that they are tilted with respect to the lamella normal. This is a piece of evidence that crystallographic slip is actually operating[11–15]. For $\lambda \geq 3.0$, the S.A.X.S.

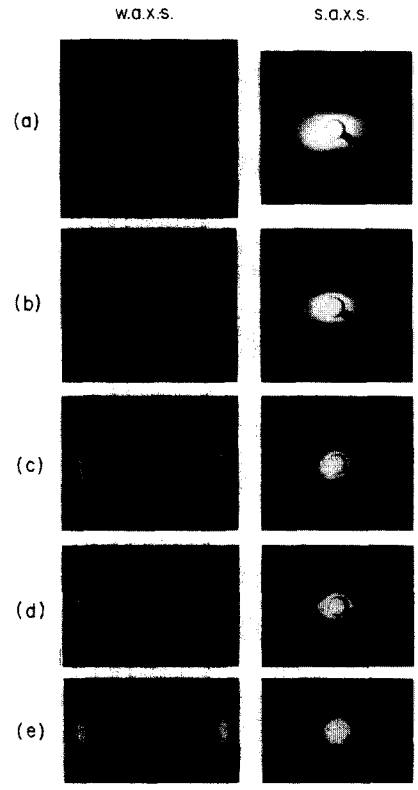

Figure 3 W.A.X.S. and S.A.X.S. patterns of copolymer A for the draw temperature $T_d = 80°C$, as a function of draw ratio: (a) $\lambda = 1.4$, (b) $\lambda = 1.8$, (c) $\lambda = 3.0$, (d) $\lambda = 4.0$, (e) $\lambda = 5.0$ (draw axis vertical)

diffraction turns into meridional reflections. The concomitance with the orientation of the chains parallel to the draw direction, as judged from the W.A.X.S. analysis, is an indication of the occurrence of the fibrillar transformation, a well known phenomenon in polyethylene[16]. The fibre-like structure undergoes significant improvement with increasing draw ratio as revealed by the gradual change of the arched meridional reflections into horizontal streaks, in parallel to the azimuthal narrowing of the equatorial W.A.X.S. reflections.

Figure 3 shows the W.A.X.S. and S.A.X.S. patterns of copolymer A samples drawn at $T_d = 80°C$, as a function of draw ratio. The (110) and (200) reflections display quadrant and equatorial evolutions, respectively, as in the previous case for $T_d = 120°C$. However, the disappearance of the (200) reflection and the broadening of the (110) one at $\lambda \approx 4$ are more pronounced. The strain-induced disordering is much stronger at 80°C than at 120°C. Although the extinction of the (200) reflection may not seem obvious at $\lambda \geq 4$ as it merges into the (110) arc, the complete vanishing of the (100) reflection thoroughly supports a phase change process. The intensity profiles of *Figure 4* make it clear that both the (200) and the (100) reflections disappear for $\lambda \geq 4$, and that the (110) reflection slightly broadens but roughly keeps its intensity and remains at the same angular position. This confirms the strong disordering process and suggests a phase transformation of the monoclinic structure into a mesomorphic structure. The 2° half-height width of the latter unique reflection (*Figures 4d* and *4f*) is particularly consistent with a mesomorphic order, but not with an amorphous state. As a matter of fact, the half-height

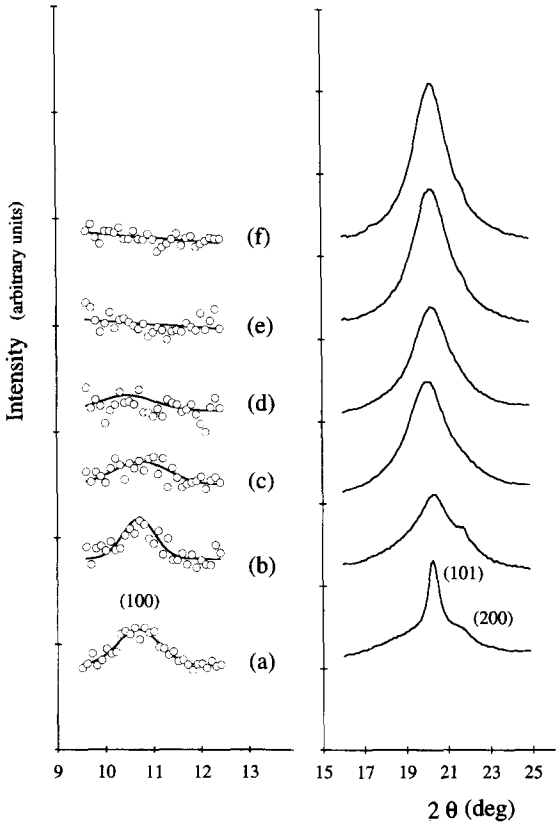

Figure 4 Equatorial W.A.X.S. intensity profiles of copolymer A for the draw temperature $T_d = 80°C$, as a function of draw ratio: (a) $\lambda = 1.0$, (b) $\lambda = 2.0$, (c) $\lambda = 3.4$, (d) $\lambda = 4.0$, (e) $\lambda = 5.0$, (f) $\lambda = 6.0$

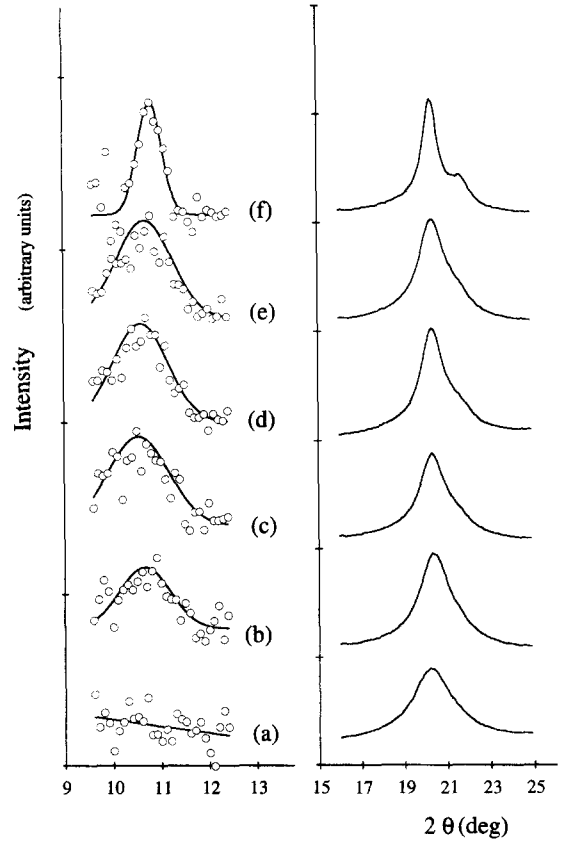

Figure 5 Equatorial W.A.X.S. intensity profiles of copolymer A as a function of the draw temperature, for a draw ratio $\lambda \approx 4.0$: (a) $T_d = 80°C$, (b) $T_d = 100°C$, (c) $T_d = 110°C$, (d) $T_d = 120°C$, (e) $T_d = 130°C$, (f) $T_d = 140°C$

broadness of an amorphous scattering halo usually lies between 4 and 6°[22,23].

The change of the S.A.X.S. patterns with strain at T_d = 80°C (*Figure 3*) is quite different from the case of T_d = 120°C. Indeed, after the development of an equatorial reflection for $\lambda \leq 1.8$, the unique S.A.X.S. order gradually vanishes with increasing draw ratio. No more scattering is observed for $\lambda \geq 3$, even at exposure times of 3 days. This could be a consequence of the decrease of the density of the strain-induced mesomorphic phase down to a value close to that of the amorphous phase, as has been shown by Fischer and Fakirov[24] in the case of drawn PET. This may as well result in part from the densification of the amorphous phase upon orientation as it is the case for PVOH[25].

The intensity W.A.X.S. profiles of copolymer A samples drawn up to $\lambda \approx 4$ at various draw temperatures are reported in *Figure 5*. Despite the gradual broadening of the (200) reflection with decreasing T_d, the two stronger (110) and (200) reflections of the monoclinic structure remain clearly observable until T_d = 110°C. Besides, the (110) reflection is not very sharp at T_d = 140°C, i.e. about one degree wide at half-height. It seems to be a general trend of EVOH and PVOH to display rather broad crystalline reflections, in the drawn state as well as in the isotropic state[26,27]. This phenomenon is indicative of the presence of rather small crystals.

The W.A.X.S. and S.A.X.S. patterns of copolymer DC samples drawn up to $\lambda \approx 6$ are reported in *Figure 6* for draw temperatures of 150° and 80°C. The same phenomenon of strain-induced disorder at T_d = 80°C is observed indicating that this is a general trend of EVOH copolymers having a high vinyl alcohol content.

Figure 7 shows the W.A.X.S. patterns of copolymer A fibres drawn at 80 and 150°C, at the same draw ratio $\lambda \approx 6$, for short and long exposure times in order to compare the zeroth diffraction level (hk0), i.e. the equatorial diffraction of the fibre structure, and the first diffraction level (hk1). From the short exposure patterns of *Figure 7*, it can be seen that the disordered structure is well-established at T_d = 80°C, while the monoclinic structure is preserved at T_d = 150°C, in the highly oriented material. In the long exposure patterns of *Figure 7*, which both resemble the fibre diagrams of monoclinic PVOH[28], the first diffraction level is only slightly affected by the draw temperature. This is a piece of evidence that a crystal-like order persists in the disordered structure induced at low draw temperature, and rules out the hypothesis of amorphization that has been previously discussed[26]. The quite similar azimuthal dispersion of the spots for the two patterns recorded at long exposure indicates that chain orientation is little sensitive to the draw temperature and mainly depends on the draw ratio. The vanishing of the higher equatorial orders, notably the (020) reflection, in the pattern of the sample drawn at T_d = 80°C is consistent with the loss of lateral ordering previously judged from the vanishing of the (200) reflection. These findings are in favour of a smectic-like order, as pointed out by Saraf and Porter[29] who have observed a similar phenomenon for uniaxially oriented polypropylene.

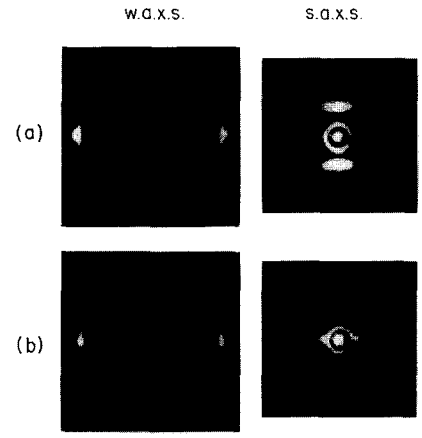

Figure 6 W.A.X.S. and S.A.X.S. patterns of copolymer DC for the draw temperatures (a) T_d = 150°C and (b) T_d = 80°C, at the draw ratio $\lambda \approx 6$ (draw axis vertical)

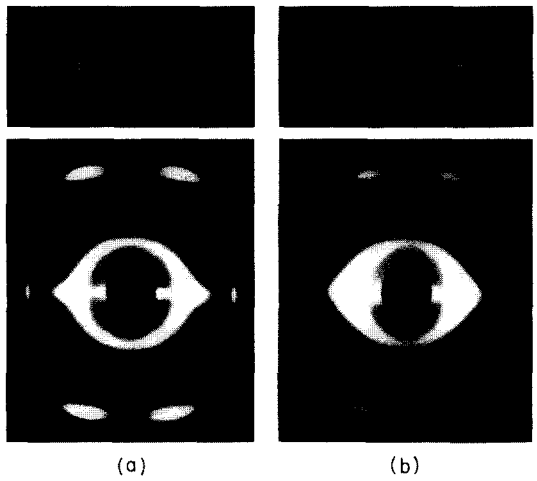

Figure 7 W.A.X.S. patterns of copolymer A drawn up to the draw ratio $\lambda \approx 6$, for the draw temperatures (a) T_d = 150° and (b) T_d = 80°C: (upper row) short exposure, (lower row) long exposure (draw axis vertical)

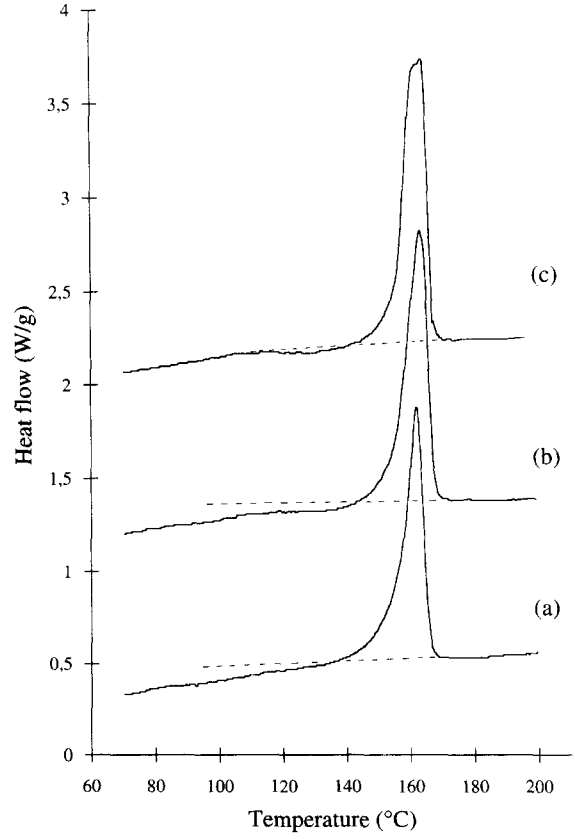

Figure 8 d.s.c. heating curves of copolymer A for the draw temperature T_d = 120°C, as a function of draw ratio: (a) λ = 2.0, (b) λ = 4.0, (c) λ = 6.0

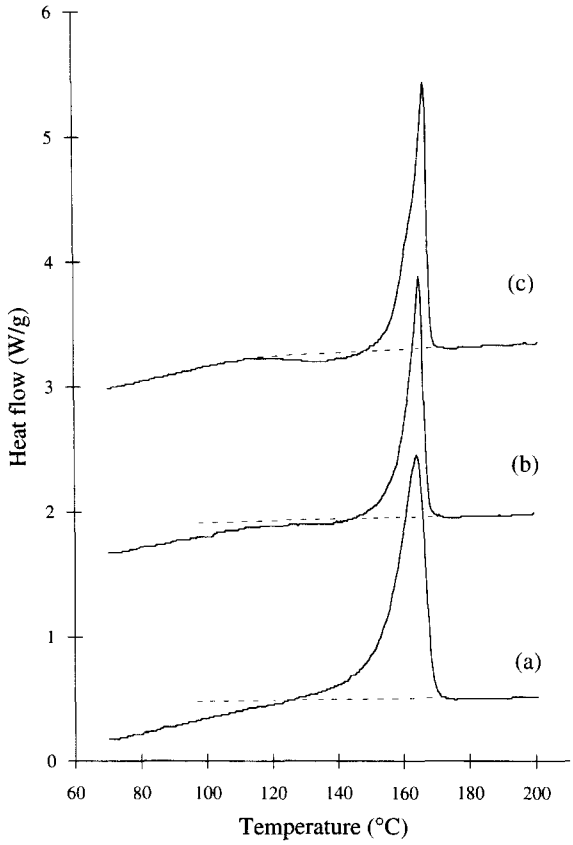

Figure 9 d.s.c. heating curves of copolymer A for the draw temperature $T_d = 80°C$, as a function of draw ratio: (a) $\lambda = 2.0$, (b) $\lambda = 4.0$, (c) $\lambda = 6.0$

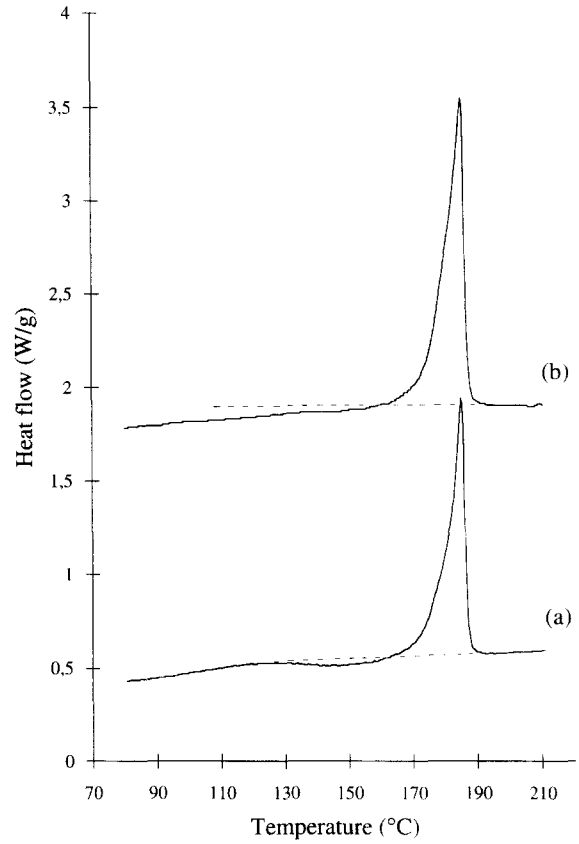

Figure 10 d.s.c. heating curves of copolymer DC for the draw temperatures (a) $T_d = 80°C$ and (b) $T_d = 140°C$, at the draw ratio $\lambda \approx 6$

Thermal characterization

The d.s.c. curves of *Figures 8* and *9* show a clear cut difference in the melting behaviour of copolymer A samples drawn at 120 and 80°C. At the draw temperature $T_d = 120°C$, the sharp melting endotherm displays minor changes with the increase of draw ratio. On the contrary, the samples drawn at $T_d = 80°C$ exhibit a significant modification at about $\lambda \approx 4$. For the samples drawn below this strain threshold the melting peak is roughly similar to that of the isotropic material. The endotherm of very weak amplitude spanning the range 60–110°C is relevant to the vaporization of some remaining humidity that has not been released during the drawing process or by the drying treatment. Beyond $\lambda = 4$, an exotherm appears over the range 110–150°C. The coincidence of the onset temperature with that of the α relaxation[10] strongly suggests a reorganization process within the crystalline component of the material owing to the activation of the molecular mobilities in this phase. Besides, the exothermic character of the transition argues for a phase change towards a thermodynamically more stable form, i.e. an improvement of phase order. According to the W.A.X.S. analysis, the smectic-like phase that is strain-induced at $T_d = 80°C$ for $\lambda \geq 4$ does not appear at $T_d = 120°C$ for the same draw ratio. Therefore we may suspect that it is not stable above about 110°C and will be prone to revert back to the monoclinic form. It is worth noticing that an analogous exothermic transition has been observed for compression-drawn[30,31] as well as quenched PP[29,32,33]. A first order smectic-to-crystal transition has been proposed by Saraf and Porter[29].

The fact that the mesomorphic structure can be induced at high draw ratio $\lambda = 6.0$ in the samples drawn at 120°C, i.e. about 10° above the transition temperature, may be ascribed to the strain-hardening that enforces increasing stresses and consequently higher local disorder on the crystalline chains. The subsequent quick cooling of the samples down to room temperature after drawing, i.e. below T_g, quenches the unstable disordered crystallites. For the sake of comparison, it deserves to be mentioned that the smectic form of PP can also be mechanically promoted at deformation temperatures above the normal transition temperature provided that the strain rate is high enough[30].

The d.s.c. curves of copolymer DC samples drawn up to $\lambda \approx 6$ are reported in *Figure 10* for the draw temperatures of 140 and 80°C. The exothermic peak ascribed to the reorganization of the smectic phase into monoclinic phase for the sample drawn at $T_d = 80°C$ is less obvious than in the case of copolymer A at equivalent draw conditions (*Figure 9c*) because of the broad endotherm of vaporisation of the residual sorbed water. Copolymer DC is more water-sensitive than copolymer A owing to a greater vinyl alcohol comonomer content and the drying treatment is not efficient enough to remove all the water. Nevertheless, the d.s.c. data on copolymer DC confirm that the strain-induced disorder at low draw temperature is not specific to copolymer A.

Annealing treatment

Strain-induced low-order phases or mesomorphic structures have been already reported for poly(ethylene terephthalate)[34–36] drawn below the glass transition temperature and for polypropylene[30,31] compressed below 70°C. The present structural change in EVOH induced by drawing is rather related to that reported for PP since the new mesomorphic structure is stable far above T_g.

Free-end samples have been annealed, for 1 min, in the

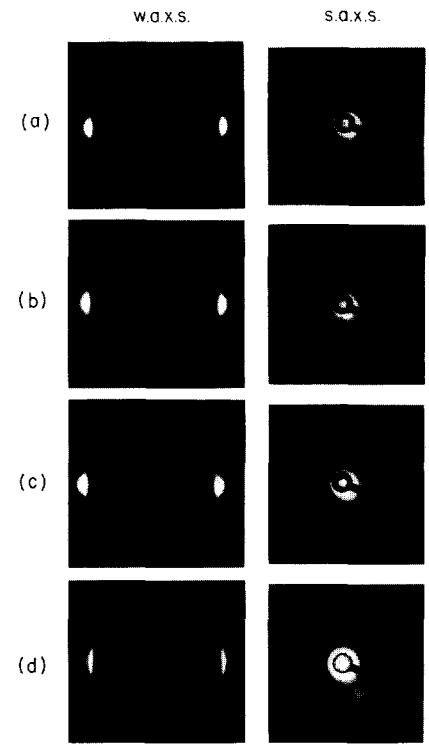

Figure 11 W.A.X.S. and S.A.X.S. patterns of copolymer A drawn up to $\lambda \approx 5$ at the draw temperature $T_d = 80°C$, then annealed for 1 min with free ends at (a) 100°, (b) 110°, (c) 120° and (d) 130°C (draw axis vertical)

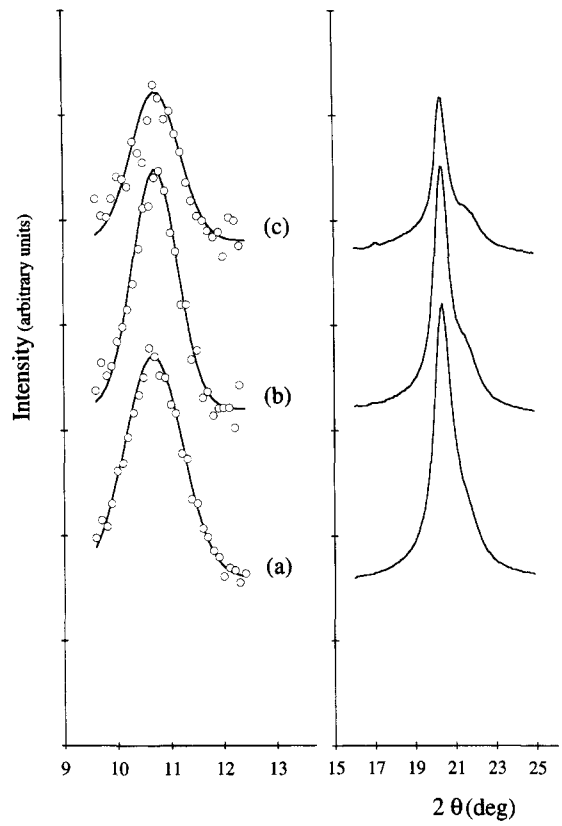

Figure 12 Equatorial W.A.X.S. intensity profiles of copolymer A drawn up to $\lambda \approx 5$ at the draw temperature $T_d = 80°C$, then annealed for 1 min with free ends at (a) 100°, (b) 110° and (c) 120°

temperature range 100–130°C in order to investigate their ability to reorganize. The W.A.X.S. patterns of *Figure 11* show that the disordered structure developed upon drawing at $T_d = 80°C$ remains unaltered upon annealing at 100°C. But annealing above 110°C regenerates the original monoclinic crystalline phase within 1 min. The intensity profiles of *Figure 12* emphasize this recovery of the stable crystalline form by the clear appearance of the (100) and (200) reflections. The α mechanical relaxation to which we have previously attributed the reverse structural transition (see Section 3.2 'Thermal Characterization' and Ref. 10) thanks to the activation of the molecular mobilities in the crystalline phase is not a thermodynamic transition. Therefore it cannot be directly responsible for the exothermic transition but is precursory of it.

Worth noticing is the drop of intensity of the main (110) reflection of the drawn sample annealed at 120°C (*Figure 12c*). This is due to the relaxation of chain orientation that increases the azimuthal dispersion at the expense of the equatorial intensity.

A striking recovery of the S.A.X.S. patterns can be seen in *Figure 11* for $T_a \geq 110°C$, i.e. just about the temperature of the α relaxation in the crystal. Considering the major influence of the electron-density contrast between the ordered and amorphous phases on the scattering intensity, this finding is relevant to a reorganization of the strain-induced mesomorphic structure into a more ordered phase owing to the activation of molecular mobilities at 110°C. Conversely, this provides support to our interpretation that the S.A.X.S. intensity drop that occurs upon drawing at $T_d =$ 80°C originates from the crystal disordering at temperature where molecular mobility is not high enough to restore the stable monoclinic form. The direct consequence of the loss of S.A.X.S. for the mesomorphic structure is that its density should be close to that of the amorphous phase. This will be checked below.

Quenching experiments

Matsumoto et al.[19] have reported that EVOH copolymers having vinyl alcohol molar concentrations in the range 30–40% exhibit less W.A.X.S. reflections than copolymers beyond or below this range which display the characteristic reflections of orthorhombic PE and monoclinic PVOH, respectively. These authors ascribed a hexagonal structure of high symmetry to the copolymers belonging to the intermediate composition range. Unfortunately, the samples were studied in the drawn state and no indication was given of the drawing conditions. One is therefore unable to conclude whether such a structure is the stable crystalline form of the copolymers or a strain-induced form as in the present study.

One should also mention that, as in polypropylene, polyamide 6 has been also reported to involve concomitant structural and mechanical changes when drawn above a critical draw rate[37]. Although the strain-induced crystalline disorder has not been clearly established in this latter case, it is well-known that polyamide 6 can develop a mesomorphic structure upon quenching[38,39].

Borrowing from the analogy with PP and polyamide 6 that are disorder-prone upon quenching, and considering that the α relaxation temperature is a key parameter in the reorganization process of EVOH copolymers, we have carried out quenching experiments below this critical temperature in order to induce the disordered phase in the isotropic materials.

Figure 13 shows the W.A.X.S. patterns of the samples of copolymer A quenched from the melt at 0°C and 60°C. Both patterns exhibit a single diffraction ring indicative of strong crystalline disorder. The narrowness of the ring rules out the possibility of a purely amorphous material. But one cannot

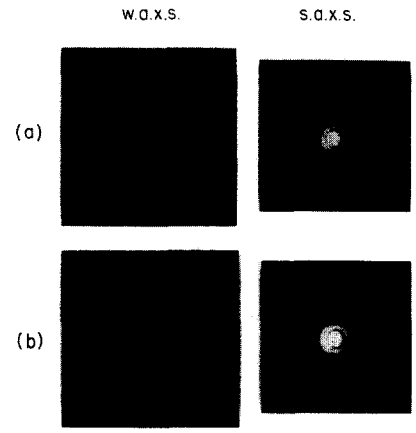

Figure 13 W.A.X.S. and S.A.X.S. patterns of copolymer A quenched from the melt into water at (a) 0° and (b) 60°C

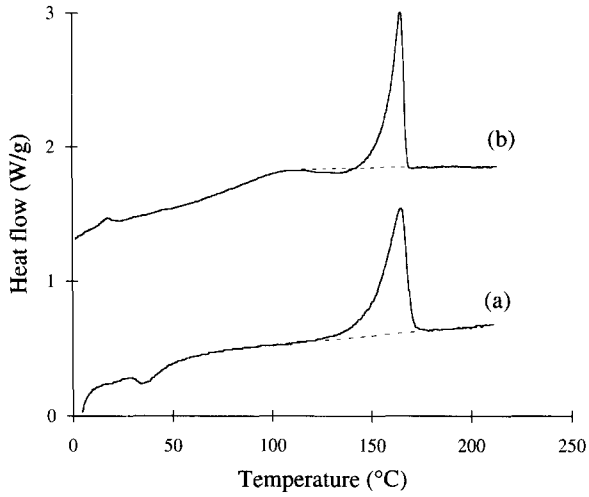

Figure 14 d.s.c. heating curves of copolymer A quenched from the melt into water at (a) 0° and (b) 60°C

distinguish between small imperfect crystals and mesomorphic entities. The absence of a diffraction ring in the S.A.X.S. patterns of *Figure 13*, compared with the slow cooled material (*Figure 1*), is rather in favour of the second hypothesis, in consideration that it should involve a drop of electron density of the mesomorphic structure compared with the monoclinic structure. However, it does not exclude highly defective crystals having a strongly reduced density.

The d.s.c. curves of the quenched samples are reported in *Figure 14*. Quenching into water at 0°C partly inhibits crystallization as revealed by the weak recrystallization peak at about 40°C, i.e. just above the glass transition temperature. No exotherm is observed in the range 110–130°C. Therefore, the structure is more likely made of small imperfect crystals that may undergo a gradual improvement of perfection during the heating scan, as has often been reported for polymers of low crystallization rate. In the case of quenching into water at 60°C, an exotherm is visible in the range 110–130°C of the d.s.c. curve which is relevant to the presence of the mesomorphic phase. In this case, the cooling step is obviously fast enough to prevent crystallization into the monoclinic form but does not allow the molten polymer to be frozen in the amorphous state thanks to the temperature of the water bath being above the glass transition.

Attempts to induce the mesomorphic structure in isotropic copolymer DC by quenching have failed. The

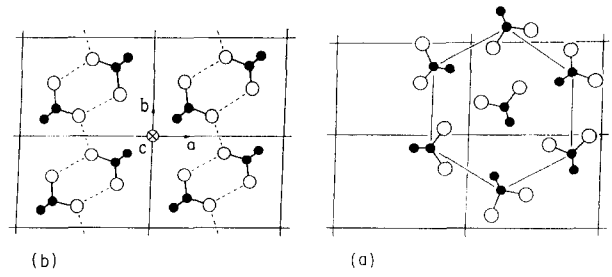

Figure 15 Model for (a) the mesomorphic unit cell as compared to (b) its mother monoclinic unit cell (see text for details)

W.A.X.S. patterns as well as the d.s.c. traces did not disclose significant amount of mesomorphic phase. It seems that copolymer DC has a greater ability for crystallizing in the sheet-like structure than copolymer A, owing to a higher vinyl alcohol content. Small imperfect crystals may eventually be formed.

Mesomorphic phase model

Figure 15 shows the unit cell that is assumed for the mesomorphic structure in comparison with the mother monoclinic structure. The position of the chains are only slightly changed with respect to the monoclinic unit cell. The main change is the random orientation of the hydroxyl groups about the chain axis which prevents the build-up of a sheet-like structure. It necessarily involves a conformational disorder along the chains, the so-called condis crystal, that only allows a short-range crystalline organization. This random distribution of the hydroxyl groups favours organization of the chains into a highly symmetric unit cell, namely hexagonal, owing to the isotropy of the interchain interactions. This new symmetry implies that the original (110) and (200) crystallographic planes of the monoclinic unit cell become equivalent, involving a unique X-ray reflection.

From the Bragg spacing of the unique reflection associated with the main (100) hexagonal planes, one may determine the density of the mesomorphic phase, $\rho_{meso} \approx 1.29\ g\ cm^{-3}$. This value is significantly lower than that of the monoclinic crystal, $\rho_{mono} = 1.35\ g\ cm^{-3}$ [23], but compares very well with that of the amorphous phase[22]. This finding provides a definitive explanation for the loss of S.A.X.S. of the samples in the mesomorphic state induced by drawing at 80°C or by quenching, since the S.A.X.S. intensity is proportional to the square of the difference of electronic densities between the two phases, namely either crystalline–amorphous or mesomorphous–amorphous.

The crystal-locked conformational defects along the chain stems deserve a particular comment, in relation to the random distribution of the H-bonds. In the case of drawing below 110°C, the sheet-like structure of the monoclinic crystalline phase (*Figure 15*) is disrupted by the crystallographic slip processes during the course of plastic deformation. The stress-induced chain defects such as twists or kinks that allow crystal slip put the chains out of crystallographic register. The latter cannot rebuild after drawing because of the lack of molecular mobility in the crystal. The chains may yet find metastable settlement in the potential energy minima of the mesomorphic structure. Interchain H-bonds are allowed to form again, but in a random fashion about the chain axis.

When induced in the isotropic state by an appropriate quenching treatment, the disordered phase is suspected to

result from a kinetic effect. If the cooling rate is not drastically fast, the chains are allowed to fold back and arrange themselves roughly parallel to each other before immobilization when temperature goes below 110°C. As a matter of fact, for cooling rates of 10, 40 and 100° min^{-1}, the crystallization peak temperatures are 143, 135 and 118°C, respectively. So, for cooling rates of a few tens of degrees s^{-1} that can be reached upon quenching, T_c may lie in the temperature range of the α mechanical relaxation, or even below it, thus preventing the final local arrangement of the chains in the all-*trans* conformation that is characteristic of the monoclinic stable form. But it is mandatory to stop the quick cooling step before the glass transition temperature in order to prevent solidification in the amorphous state.

This interpretation is consistent with the suggestion of Wunderlich and Grebowicz[40] that the mesomorphic structure of quenched polymers which usually crystallize from the melt can be considered as an intermediate stage in the crystallization pathway.

Regarding the thermal behaviour of the samples which display a mesomorphic structure from W.A.X.S., the occurrence of an exothermic peak prior to the melting peak has been taken as a piece of evidence of a reorganization process. However, the endothermic heat capacity jump preceding the exotherm has not been attributed a clear cut origin. In the case of smectic polypropylene, the assignment to the premelting of imperfect crystals[32,33] is unsatisfactory as long as the smectic order is assumed. As a tentative explanation, one may consider that reaching the temperature of the α crystalline relaxation during the heating scan involves activation of molecular mobilities which allow first a kind of smectic-to-nematic transition accompanied by a heat capacity increase. Then, the chain mobility turns out high enough to allow recrystallization of the transient nematic-like copolymer into its stable monoclinic form.

Mechanism of the strain-induced transformation

The presence of nearly unperturbed first-order strata in the W.A.X.S. fibre pattern of *Figure 7b* is indicative of a strong crystalline order in the chain direction. The major modification lies in the loss of the lateral packing. One may first suspect crystallographic slip parallel to the chain axis, i.e. the so-called chain slip, to be responsible for the disorganization effect. Indeed, stress-activated conformational defects in the chains are necessary for the crystallographic slip to proceed since complete crystal stem migration is unrealistic. These defects may remain frozen in the crystal below the temperature of the α relaxation which is the threshold of activation of the molecular mobilities in the crystal. This phenomenon is likely to randomize the H-bond distribution about the chain axis. However, this destructuring effect should occur as soon as plastic deformation starts since plasticity takes place through the build up of a stock of crystalline defects that culminates at the yield point before their propagation at nearly constant defect density. This is contrary to the observed facts.

As an alternative assumption, it is suggested that crystallographic slip normal to the chain axis, otherwise transverse slip, is the relevant mechanism of the phase change. Such a kind of crystal slip is indeed able to modify the lateral packing of the chains in the crystal, i.e. the unit cell basal plane, without changing significantly the longitudinal order. This can be judged for instance from PE[41,42] which displays a strain-induced phase change from the orthorhombic to the monoclinic form. However, transverse b-slip or a-slip in EVOH involve greater Burgers vector and consequently higher critical shear stress than the chain slip, i.e. c-slip (see *Figure 15*). Then, as deformation proceeds, the strain-hardening due to chain unfolding involves a tensile stress increase up to such a level that the critical resolved shear stress is reached in the slip planes able to induce phase change. This is perfectly consistent with the observation of a strain threshold for the appearance of the disordered phase. The magnitude of the critical strain has yet to be understood. It is worth noticing that transverse a-slip is more likely to result in a phase change since it crosses the H-bonds and is therefore able to alter the cohesion of the sheet structure of the monoclinic crystal cell.

CONCLUSION

The structural evolution of EVOH copolymers upon tensile drawing strongly depends on the draw temperature. Above the temperature of the α relaxation, i.e. about 110°C, the crystalline phase is able to reorganize into the stable monoclinic form during the course of plastic deformation. But below this critical temperature, the crystalline phase suffers a disorganization into a mesomorphic state of the smectic type. This strain-induced transformation is characterized by a disruption of the sheet-like structure of the monoclinic form. This is a consequence of the stress-activation of crystal plasticity defects and inhibition of the molecular mobilities associated with the α relaxation.

Quenching experiments carried out on thin films show that the mesomorphic state can be thermally-induced in the isotropic materials. It seems to be a metastable stage in the pathway to crystallization that is frozen in by rapid cooling.

The random distribution of hydrogen bonds about the chain axis in the mesomorphic form provides mechanical isotropy at the scale of the crystal unit cell. The resulting structure is more ductile and less fissure-prone than the sheet-like monoclinic form.

ACKNOWLEDGEMENTS

The authors are indebted to ELF-ATOCHEM for financial support and for permission to publish this work.

REFERENCES

1. Samuels, R. J., *Structured Polymer Properties*. Wiley Interscience, New York, 1974.
2. Ward, I. M., ed., *Structure and Properties of Oriented Polymers*. Applied Science, London, 1975.
3. Ward, I. M., ed., *Developments in Oriented Polymers*, Vol. 1. Applied Science. London, 1982.
4. Zachariades A. E. and Porter, R. S., editors. *Strength and Stiffness of Polymers*. Marcel Dekker, New York, 1983.
5. Ohta, T., *Polym. Eng. Sci.*, 1983, **23**, 697.
6. Gogolewski, S. and Pennings, A. J., *Polymer*, 1985, **26**, 1394.
7. Ito, M., Tanaka, K. and Kanamoto, T. J., *Polym. Sci., Polym. Phys. Ed.*, 1987, **25**, 2127.
8. Cebe, P. and Grubb, D. J., *J. Mater. Sci.*, 1985, **20**, 4465.
9. Hong, P.-D. and Miyasaka, K., *Polymer*, 1991, **32**, 3140.
10. Djezzar, K., Penel, L. Lefebvre, J.-M., Seguela, R. and Germain, Y., *Polymer*, 1998, **39**, 3945.
11. Peterlin, A. and Meinel, G., *Makromol. Chem.*, 1971, **142**, 227.
12. Robertson, R. E., *J. Polym. Sci., Polym. Phys. Ed.*, 1971, **9**, 1255.
13. Takayanagi, M. and Kajiyama, T., *J. Macromol. Sci., Phys.*, 1973, **B8**, 1.
14. Kambour, R. P. and Robertson, R. E., in *Polymer Science*, ed. A. D. Jenkins. North–Holland, London, 1972, Chapter 11.

15. Bowden, P. B. and Young, R. J., *J. Mater. Sci.*, 1974, **9**, 2034.
16. Alexander, L. E., *X-Ray Diffraction Methods in Polymer Science*. Wiley–Interscience, New York, 1969, Chapter 5.
17. The indexation adopted for the monoclinic reflexions of EVOH is the one assuming the c axis parallel to the chain axis.
18. Matsumoto, T., Nakamae, K., Ogoshi, N., Kawasoe, M. and Oka, H., *Kobunshi Kagaku*, 1971, **28**, 610.
19. Matsumoto, T., Nakamae, K., Oka, H. and Kawarai, S., *Sen-i-Gakkaishi*, 1974, **30**, 391.
20. Matsumoto, T., Nakamae, K., Ochiumi, T., Kawarai, S. and Shioyama, T., *Sen-i-Gakkaishi*, 1977, **33**, 49.
21. Harrison, I. R., Kozinski, S. J., Varnell, W. D. and Wang, J. I., *J. Polym. Sci., Polym. Phys. Ed.*, 1981, **19**, 487.
22. Wilchinsky, Z. W., *J. Polym. Sci., Polym. Phys. Ed.*, 1968, **6**, 281.
23. Wunderlich, *Macromolecular Physics, Vol.1, Crystal Structure, Morphology, Defects*, Academic Press, New York, 1973, Chapter 4.
24. Fischer, E. W. and Fakirov, S., *J. Mater. Sci.*, 1976, **11**, 1041.
25. Hong, P.-D. and Miyasaka, K., *Polymer*, 1994, **35**, 1369.
26. Yoshida, H., Tomizawa, K. and Kobayashi, Y., *J. Appl. Polym. Sci.*, 1979, **24**, 2277.
27. Sato, T. and Okaya, T., *Polym. J.*, 1992, **24**, 849.
28. Tadokoro, H., *Structure of Crystalline Polymers*. Wiley–Interscience, New York, 1979, p. 153-154.
29. Saraf, R. and Porter, R. S., *Mol. Cryst. Liq. Cryst. Lett.*, 1985, **2**, 85.
30. Saraf, R. F. and Porter, R. S., *Polym. Eng. Sci.*, 1988, **28**, 842.
31. Osawa, S. and Porter, R. S., *Polymer*, 1994, **35**, 545.
32. Vittoria, V., *J. Macromol. Sci., Phys.*, 1989, **B28**, 97.
33. Fichera, A. and Zannetti, R., *Makromol. Chem.*, 1975, **176**, 1885.
34. Armeniades, C. D. and Bear, E., *J. Polym. Sci., Polym. Phys. Ed.*, 1971, **9**, 1345.
35. Lindner, W. L., *Polymer*, 1973, **14**, 9.
36. Sun, T., Zhang, A., Li, F. M. and Porter, R. S., *Polymer*, 1988, **29**, 2115.
37. Pakula, T. and Fischer, E. W., *J. Polym. Sci., Polym. Phys. Ed.*, 1981, **19**, 1705.
38. Ziabicki, A. and Kolloid, Z. Z., *Polym.*, 1959, **167**, 132.
39. Murthy, N. S., *Polymer Comm.* 1991, **32**, 301. (see Wunderlich, Chapter 4.).
40. Wunderlich, B. and Grebowicz, J., *Adv. Polym. Sci.*, 1984, **60/61**, 1.
41. Kiho, H., Peterlin, A. and Geil, P. H., *J. Appl. Phys. Ed.*, 1964, **35**, 1599.
42. Allan, P. and Bevis, M., *Proc. R. Soc. London*, 1974, **Ser. A 341**, 75.